

# Oxygen Content Effect in Y—Ba—Cu—O Superconductors

M. BREZA

Department of Chemical Physics, Faculty of Chemical Technology, Slovak Technical University, CS-812 37 Bratislava

Received 29 July 1992

The dependence of electronic structure of superconducting  $\text{YBa}_2\text{Cu}_3\text{O}_y$  on the oxygen content is investigated using the standard CNDO/2 and quasi-relativistic CNDO/1 molecular orbital method. Electronic structures of model clusters  $[\text{Cu}_3\text{O}_n]^q$  with total charges  $q = 7 - 2n$  and  $n = 11$  to 14 in various geometries are compared. Possible Cu(III) in real systems may be ascribed to penta-coordinate Cu-2 in  $\text{CuO}_2$  planes for  $y < 7$  or to Cu-1 in Cu—O chains for  $y > 7$ . The apical oxygen position within Cu-1—O-2—Cu-2 frame is influenced by actual Cu-1 coordination implied by the  $y$  value.

$\text{YBa}_2\text{Cu}_3\text{O}_y$  is the most common high-temperature superconductor. Depending on the way of preparation and on the oxygen content,  $y$ , its onset transition temperature to the superconducting state,  $T_c$ , varies [1] from ca. 55 K ( $y = 6.5$ – $6.6$ ) to ca. 93 K ( $y = 6.75$ – $6.85$ ). According to X-ray structure data [2, 3], the unit cell of superconducting  $\text{YBa}_2\text{Cu}_3\text{O}_y$  (Fig. 1) is of  $\text{D}_{2h}^1$ -Pmmm symmetry. The copper atoms are at two distinct sites corresponding to two different oxidation states. The copper-oxide planes are composed of  $(\text{Cu-2})\text{O}_5$  tetragonal pyramids connected by corner O-3 and O-4 atoms. The apical O-2 ones connect a pair of these pyramids with the

central Cu-1 atom. The averaged coordination of Cu-1 depends on the oxygen content  $y$ . The generally accepted (distorted) square-planar coordination with linear Cu-1—O-2 chains corresponds to an "ideal"  $\text{YBa}_2\text{Cu}_3\text{O}_7$  structure. Lower oxygen content causes some breaks of these chains. Moreover, the occupancy of remaining O-5 sites completing the (distorted)  $(\text{Cu-1})\text{O}_6$  octahedron is, in principle, non-vanishing [2, 3] and rises with the oxygen content  $y$ . Consequently, various models of Cu-1 coordination are possible in real  $\text{YBa}_2\text{Cu}_3\text{O}_y$  systems. Assuming constant environmental influence, the Ba and Y atoms completing the unit cell may not be considered in the simplest model systems presented in Table 1. Despite high simplicity of these models, this series of the systems of high similarity should give the same trends of properties as the more complex ones (cf. our previous results on  $[\text{Cu}_3\text{O}_{12}]^{-17}$ ,  $[\text{Ba}_8\text{Cu}_3\text{O}_{12}]^{-1}$ , and  $[\text{Y}_8\text{Cu}_3\text{O}_{12}]^{+7}$  model systems [4, 5]).

## METHOD

Electronic structure of some simple cluster models (Table 1) of  $\text{YBa}_2\text{Cu}_3\text{O}_y$  has been studied in

Table 1. Description of Model Systems of Hypothetical  $\text{YBa}_2\text{Cu}_3\text{O}_y$  with Single  $(\text{Cu-1})\text{O}_n$  Geometry

Model	$y$	Cluster	Local $(\text{Cu-1})\text{O}_n$ geometry			
			O-1	O-5		
A1	6.5	$[\text{Cu}_3\text{O}_{11}]^{-15}$	0 $b/2$ 0	—		
A2	6.5	$[\text{Cu}_3\text{O}_{11}]^{-15}$	—	$a/2$ 0 0		
B1	7.0	$[\text{Cu}_3\text{O}_{12}]^{-17}$	0 $b/2$ 0 0 $-b/2$ 0	—		
B2	7.0	$[\text{Cu}_3\text{O}_{12}]^{-17}$	0 $b/2$ 0	$a/2$ 0 0		
C1	7.5	$[\text{Cu}_3\text{O}_{13}]^{-19}$	0 $b/2$ 0 0 $-b/2$ 0	$a/2$ 0 0		
C2	7.5	$[\text{Cu}_3\text{O}_{13}]^{-19}$	0 $b/2$ 0	$a/2$ 0 0 $-a/2$ 0 0		
D	8.0	$[\text{Cu}_3\text{O}_{14}]^{-21}$	0 $b/2$ 0 0 $-b/2$ 0	$a/2$ 0 0 $-a/2$ 0 0		

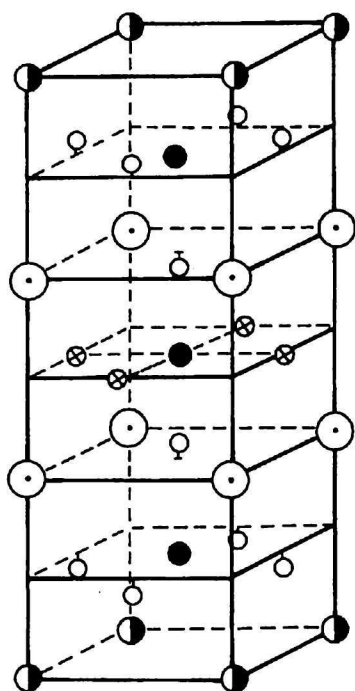


Fig. 1. The unit cell of  $\text{YBa}_2\text{Cu}_3\text{O}_y$ .  $\circ$  Ba,  $\bullet$  Y,  $\bullet$  Cu,  $\circ$  O,  $\otimes$  vacant oxygen positions.

experimental geometries [2] of the unit cell (Fig. 1). All model systems are in the singlet spin states.

MO—LCAO—SCF calculations have been carried out by the standard CNDO/2 method [6] and/or by quasi-relativistic (QR) CNDO/1 method [7] with a standard Cu reference configuration.

The problem of description of a great number of molecular orbitals in polyatomic systems may be successfully solved using the Density of States (DOS) treatment. Intensities of individual DOS peaks are proportional to electronic densities and their positions are given by corresponding orbital energies.

The DOS function may be calculated using a Gauss-type function

$$N(\varepsilon) = (2\pi\sigma)^{-1/2} \sum_i^{\text{occ}} P_i \exp [-(\varepsilon - \varepsilon_i^2) / 2\sigma^2] \quad (1)$$

where  $\sigma = 0.02 R_\infty$  is the spectral broadening parameter,  $\varepsilon_i$  are the orbital energies and  $P_i$  the projection weights ( $P_i = 1$  for the total DOS and  $0 < P_i < 1$  for the projected  $d$ -DOS depending on the portion of the  $d$ -orbitals in the individual molecular orbital) [5].

## RESULTS AND DISCUSSION

The obtained results of quantum-chemical calculations are listed in Tables 2–4 and shown in Figs. 2–6 (some figures are not presented because the DOS functions for A1 and C1 models are practically

**Table 2.** Calculated Properties of Model Systems

Model	$E/\text{eV}$	$\Delta/\text{eV}$	$d^x$	
			Cu-1	Cu-2
CNDO/2 method				
A1	+ 378.45	6.00	9.46	8.76 (2×)
A2	+ 378.42	5.93	9.45	8.76 (2×)
B1	0.00	2.17	9.02	9.09 (2×)
B2	+ 3.20	2.45	9.08	9.00 (2×)
C1	− 361.45	1.70	8.69	9.26 9.15
C2	− 361.53	1.70	8.69	9.24 9.17
D	− 705.87	2.05	8.59	9.32 9.24
QR CNDO/1 method				
A2	+ 329.97	5.48	9.90	9.50 (2×)
B1	0.00	3.66	9.68	9.69 (2×)
B2	+ 1.22	3.67	9.72	9.70 (2×)
C2	− 316.13	3.17	9.47	9.93 (2×)
D	− 618.91	5.51	9.32	9.96 (2×)

$E$  – total energy of the system related to the B1 model one,  $\Delta$  – energy separation HOMO—LUMO,  $d^x$  – total  $d$ -electron population, double occurrence of individual data is indicated in parentheses.

identical with those of A2 and C2 ones, respectively). The oxidation states of copper atoms may be attributed according to the  $d$ -electron populations,  $d^x$ . As proposed in our previous paper [4] for the standard CNDO/2 method,  $d^x > 9.8$  corresponds to Cu(I),  $9.0 < d^x < 9.2$  corresponds to Cu(II) and  $d^x \approx 8.5$  may correspond to Cu(III). The QR CNDO/1 method with standard Cu( $d^{10}s^1p^0$ ) configuration shifts these limits to higher values and so  $d^x \approx 10$  corresponds

**Table 3.** Effective Atomic Charges

Model	Cu-1	Cu-2	O-2	O-3,4	O-1	O-5
CNDO/2 method						
A1	− 1.77	− 0.75 (2×)	− 0.59 (2×)	− 1.18 (6×) − 1.21 (2×)	− 1.05	—
A2	− 1.78	− 0.75 (2×)	− 0.59 (2×)	− 1.16 (2×) − 1.20 (6×)	—	− 1.03
B1	− 0.98	− 1.00 (2×)	− 0.63 (2×)	− 1.30 (4×) − 1.32 (4×)	− 1.14 (2×)	—
B2	− 1.20	− 0.94 (2×)	− 0.63 (2×)	− 1.27 (2×) − 1.29 (4×) − 1.32 (2×)	− 1.15	− 1.13
C1	− 0.71	− 1.19 − 1.07	− 0.68 (2×)	− 1.34 (2×) − 1.37 (6×)	− 1.24 (2×)	− 1.29
C2	− 0.70	− 1.17 − 1.10	− 0.68 (2×)	− 1.35 (6×) − 1.39 (2×)	− 1.30	− 1.23 (2×)
D	− 0.37	− 1.40 − 1.31	− 0.69 (2×)	− 1.39 (4×) − 1.42 (4×)	− 1.34 (2×)	− 1.30 (2×)
QR CNDO/1 method						
A2	− 1.93	− 1.15 (2×)	− 0.54 (2×)	− 1.05 (2×) − 1.11 (6×)	—	− 0.93
B1	− 1.21	− 1.49 (2×)	− 0.34 (2×)	− 1.22 (4×) − 1.29 (4×)	− 1.04 (2×)	—
B2	− 1.38	− 1.50 (2×)	− 0.33 (2×)	− 1.20 (2×) − 1.24 (2×) − 1.28 (2×) − 1.32 (2×)	− 0.96	− 0.93
C2	− 0.92	− 1.78 (2×)	− 0.47 (2×)	− 1.37 (6×) − 1.39 (2×)	− 0.58	− 1.03 (2×)
D	− 0.64	− 1.90 (2×)	− 0.43 (2×)	− 1.40 (4×) − 1.42 (4×)	− 1.10 (2×)	− 1.10 (2×)

Multiple occurrence of individual data is indicated in parentheses.

**Table 4.** Calculated Wiberg Indices  $W_{\text{Cu—O}}$ 

Model	Cu-1			Cu-2	
	O-2	O-1	O-5	O-2	O-3,4
CNDO/2 method					
A1	1.20 (2×)	1.19	—	0.63 (2×)	1.01 (6×) 0.98 (2×)
A2	1.18 (2×)	—	1.18	0.63 (2×)	1.03 (2×) 1.00 (6×)
B1	1.10 (2×)	1.02 (2×)	—	0.60 (2×)	0.86 (4×) 0.83 (4×)
B2	1.02 (2×)	0.96	0.99	0.68 (2×)	0.88 (4×) 0.84 (4×)
C1	0.92 (2×)	0.93 (2×)	0.86	0.70 (2×)	0.76 (2×) 0.78 (4×) 0.81 (2×)
C2	0.92 (2×)	0.84	0.95 (2×)	0.70 (2×)	0.75 (2×) 0.78 (2×) 0.80 (4×)
D	0.57 (2×)	0.80 (2×)	0.89 (2×)	0.87 (2×)	0.75 (4×) 0.72 (4×)
QR CNDO/1 method					
A2	1.10 (2×)	—	1.24	0.64 (2×)	0.88 (6×) 0.90 (2×)
B1	0.78 (2×)	1.05 (2×)	—	0.56 (2×)	0.82 (4×) 0.84 (4×)
B2	0.77 (2×)	1.08	1.09	0.54 (2×)	0.82 (4×) 0.84 (4×)
C2	0.88 (2×)	0.68	0.82 (2×)	0.42 (2×)	0.76 (2×) 0.80 (6×)
D	0.69 (2×)	0.72 (2×)	0.73 (2×)	0.57 (2×)	0.75 (4×) 0.73 (4×)

Multiple occurrence of individual data is indicated in parentheses.

to Cu(I),  $d^x \approx 9.6$  corresponds to Cu(II) (and  $d^x \approx 9.2$ – $9.3$  may be postulated for Cu(III)). The effective charges include the donating effect of ligands into the bonding hybrid orbitals  $s$ – $p$  so that their values may be negative. The Wiberg (bond-strength) index reflects the bond multiplicity (e.g.  $W_{\text{A—B}} = 1.0$  means that there is a single bond between atoms A and B [6]).

Both quantum-chemical methods used in this paper exhibit the most similar trends of properties of the systems under study. The exceptions may be caused by the different degree of electron density transfer from oxygen to copper atoms. The most important results may be summarized as follows:

The energy effect connected with the oxygenation decreases with the oxygen content  $y$ .

The B2 model is less stable than the standard B1 one. The A and C models exhibit vanishing isomerization energy (the reverse stability order is the artifact of the model).

The energy gap between the lowest unoccupied (LUMO) and the highest occupied (HOMO) molecular orbitals exhibits the maximal values for A models and the minimal ones for C models. The isomerization effects are of lesser importance.

The  $d^x$  values of Cu-1 decrease with the oxygen content  $y$ . Its oxidation state varies between Cu(I) and Cu(III). Analogous characteristics of Cu-2 exhibit the reverse trend.

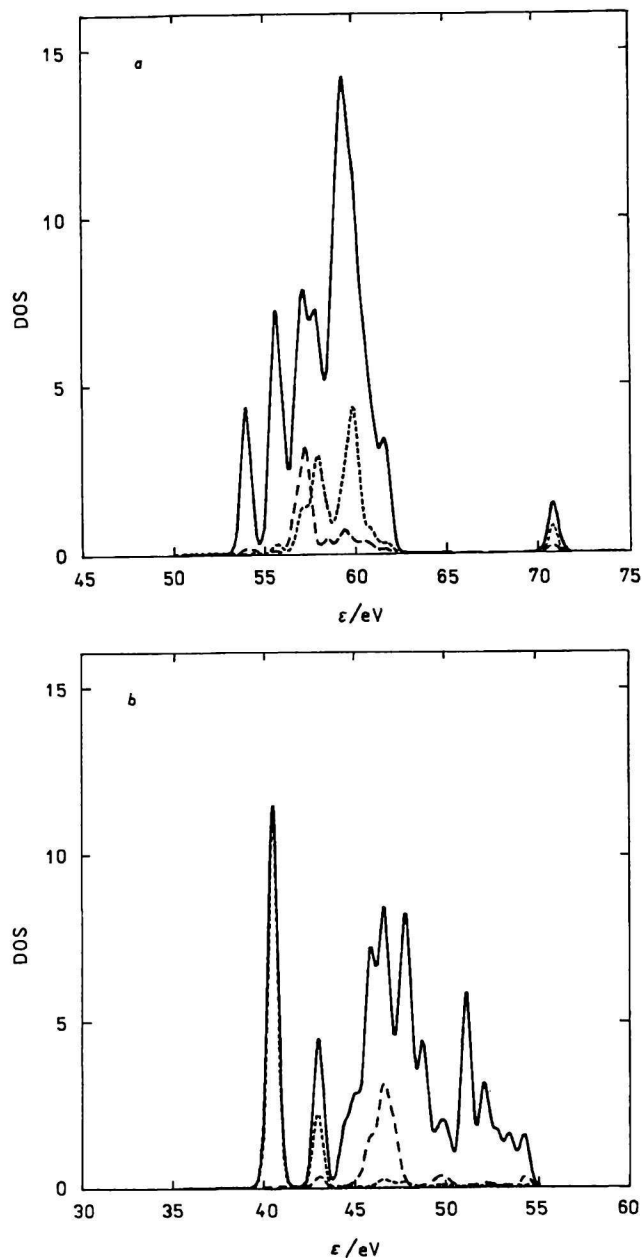


**Fig. 2.** Total DOS function (full line) and its  $d$ -projections (dashed lines) for Cu-1 (longer dashes) and Cu-2 atoms (shorter dashes) of A2 model obtained by CNDO/2 (a) and QR CNDO/1 (b) methods.

The effective atomic charges on copper atoms exhibit similar trends as the corresponding  $d^x$  values. The electron density on oxygen atoms, in general, rises with the oxygen content  $y$ . O-1 and O-5 charges are significantly influenced by the local geometry.

Cu-1—O bond strengths decrease with the oxygen content  $y$  and depend on the local geometry, too. Cu-2—O bonds (except the Cu-2—O-2 one) exhibit the similar trends.

The shape of DOS function (Figs. 2–6) significantly depends on the method of calculation. The

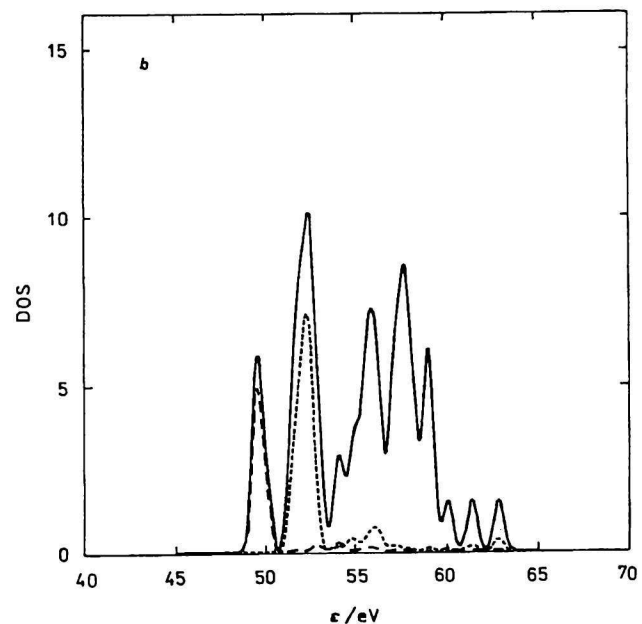
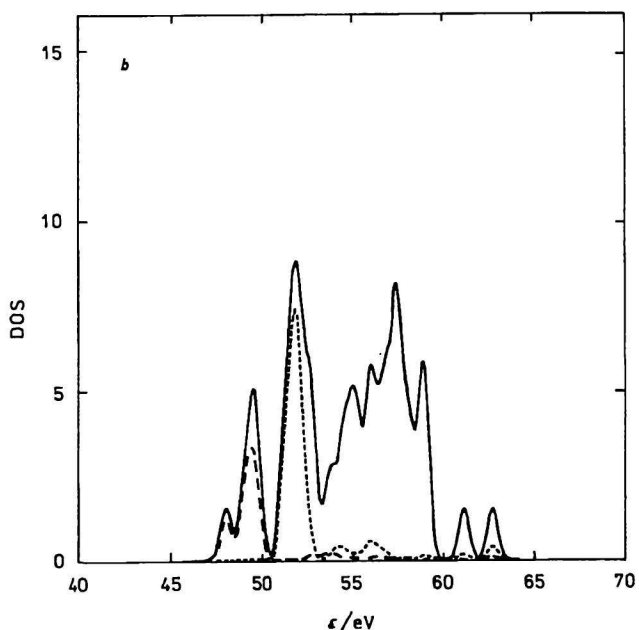
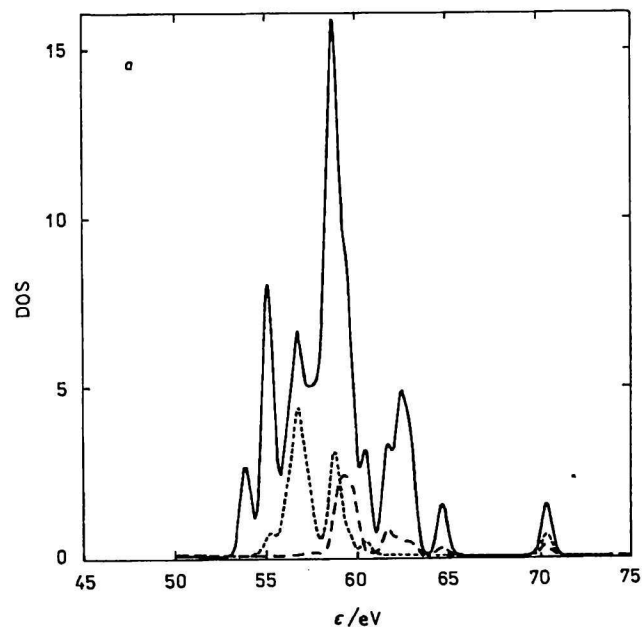
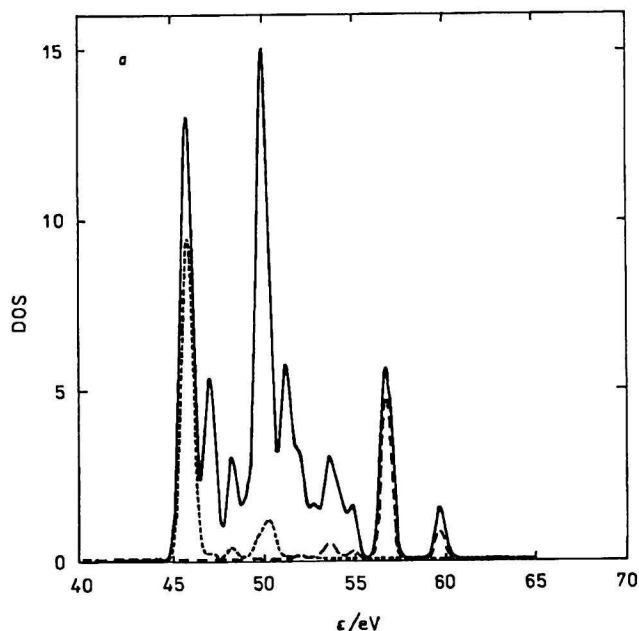


Fig. 3. The same as in Fig. 2 for the B1 model.

Fig. 4. The same as in Fig. 2 for the B2 model.

shift of maximal peaks to the higher energy edge with the increasing oxygen content  $y$  may be observed.

The positions of projected  $d$ -Cu-2 peaks (Figs. 2—6) are shifted more to the higher energy edge with the increasing oxygen content  $y$ . As a consequence, the relative positions of  $d$ -Cu-1 and  $d$ -Cu-2 bands are reversed.

A and C models (Figs. 2 and 5) exhibit the greatest difference (splitting) between maximal  $d$ -Cu-1 and  $d$ -Cu-2 peaks whereas the B models (Figs. 3, 4) exhibit the lowest one.

## CONCLUSION

According to our results, the properties of  $\text{YBa}_2\text{Cu}_3\text{O}_y$  may be significantly influenced by the oxygen content  $y$ . However, the local geometry of Cu-1 coordination within the same  $y$  value is important for the B models only ( $y = 7$ ).

Our results indicate that the possible Cu(III) existence in real systems may be ascribed to penta-coordinate Cu-2 in  $\text{CuO}_2$  layers for lower oxygen contents ( $y < 7$ ) and/or to Cu-1 in Cu—O chains for the higher ones ( $y > 7$ ). In this connection it must

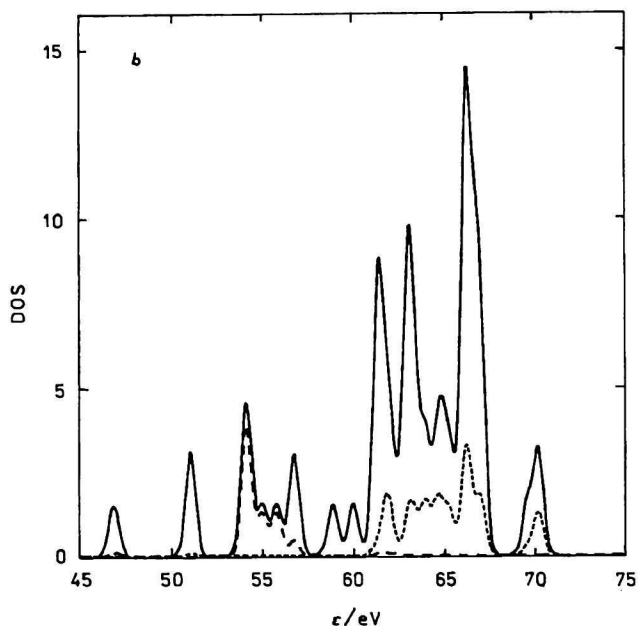
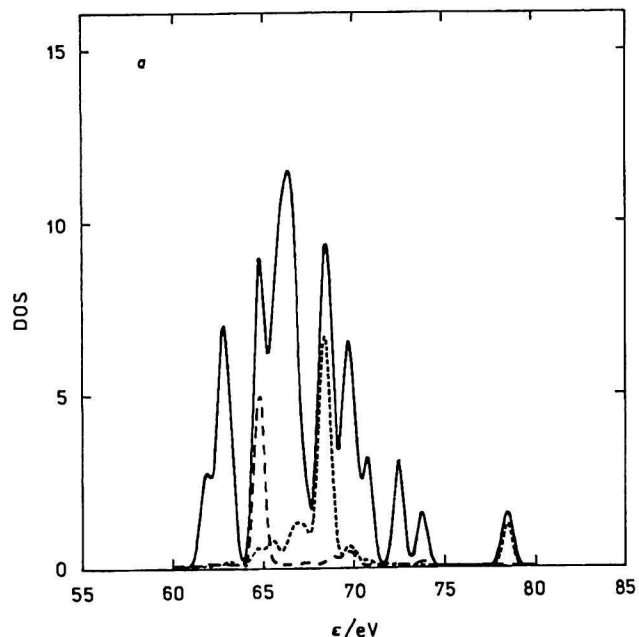


Fig. 5. The same as in Fig. 2 for the C2 model.

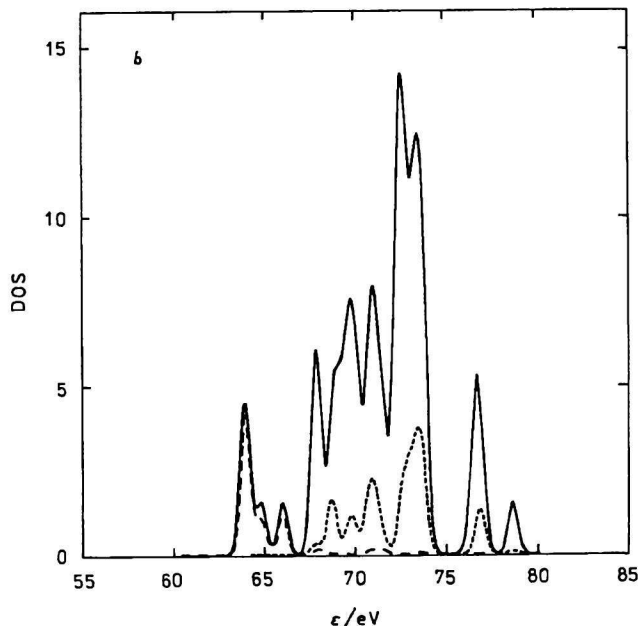
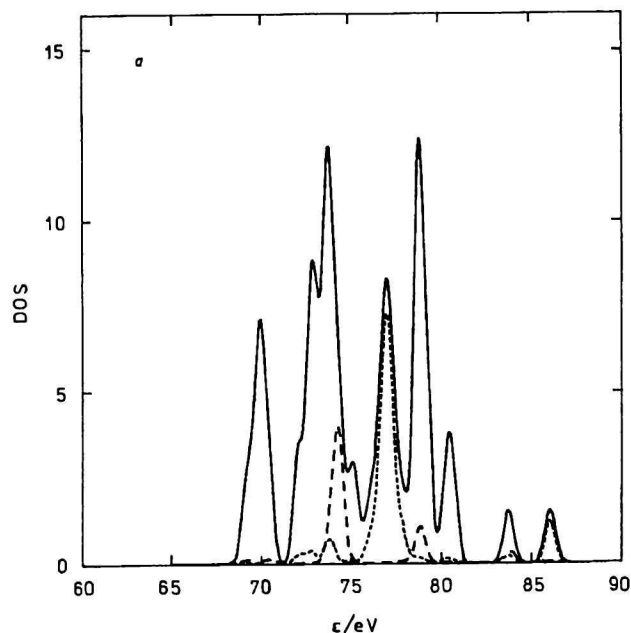


Fig. 6. The same as in Fig. 2 for the D model.

be mentioned [5] that the nonsuperconducting model cluster  $[\text{Cu}_3\text{O}_{10}]^{15-}$  exhibits only Cu(I) oxidation state due to different total charge and geometry. Thus the further condition for Cu(III) existence is the preserved electron density corresponding to the superconducting state (local charge fluctuations in real systems). This problem will be studied in some of our next papers.

As the bond lengths and bond strengths exhibit the reverse trends, the shifts of actual O-2 position between Cu-1 and Cu-2 may be deduced from the changes of Cu—O-2 bonds strengths with the ac-

tual Cu-1 coordination (realized as the local geometry fluctuations in real systems). This may be an explanation of the observed anomalies of Extended X-ray Absorption Fine Structure (EXAFS) spectra [8, 9] interpreted in terms of double-well Cu—O-2 potential. This assertion is supported by changes of average Cu—O-2 distances [1–3] with the oxygen content in real systems (some coordination types are preferred). The detailed study of this problem will be published in some of our next papers.

The results of CNDO/2 and QR CNDO/1 methods differ significantly. This is caused not only by a little

different parametrization, but mostly by inclusion of dominant relativistic effects in the latter one. Among them the orbital contraction (stabilization) of *s* and *p* orbitals as well as the indirect *d*-orbital expansion are of the greatest importance [7]. Consequently, the electron density distribution must differ especially at Cu atoms.

Due to approximations of our model systems (high negative charges, neglected Ba and Y layers) and used quantum-chemical methods, the calculated values cannot be directly compared with the experimental ones. However, as shown in our previous papers [7, 8] on more realistic models or for more sophisticated methods, the observed trends seem to be correct. Nevertheless, calculations on more extended model systems including Ba and Y atoms are in progress.

Finally it must be mentioned that bifurcation effects in our systems (nonequivalence of (Cu-2)O<sub>5</sub> polyhedra) may be explained by the so-called "symmetry dilemma" of the Hartree—Fock wave functions (the energetically best Hartree—Fock solution does not necessarily transform according to the space

symmetry of the corresponding Hamiltonian) [10, 11].

## REFERENCES

1. Whangbo, M.-H., Evain, M., Beno, M. A., Geiser, U., and Williams, J. M., *Inorg. Chem.* 27, 467 (1988).
2. Cox, D. E., Moodenbaugh, A. R., Hurst, J. J., and Jones, R. H., *J. Phys. Chem. Solids* 49, 47 (1988).
3. Jorgensen, J. D., Beno, M. A., Hinks, D. G., Soderholm, L., Volin, K. J., Hitterman, R. L., Grace, J. D., Schuller, I. K., Segre, C. U., Zhang, K., and Kleefisch, M. S., *Phys. Rev. B* 36, 3608 (1987).
4. Breza, M., *Czech. J. Phys.* 42, 191 (1992).
5. Breza, M., *Czech. J. Phys.* 42, 201 (1992).
6. Pople, J. A. and Beveridge, D. L., *Approximate Molecular Orbital Theory*. McGraw-Hill, New York, 1970.
7. Boča, R., *Int. J. Quantum Chem.* 31, 941 (1987).
8. Mustre de Leon, J., Conradson, S. D., Batistić, I. D., and Bishop, A. R., *Phys. Rev. Lett.* 65, 1394 (1990).
9. Conradson, S. D., Raistrick, I. D., and Bishop, A. R., *Science* 248, 1394 (1990).
10. Löwdin, P. O., *Rev. Mod. Phys.* 35, 496 (1963).
11. Löwdin, P. O., *Adv. Chem. Phys.* 14, 283 (1969).

Translated by M. Breza